Ind. J. Pharm. Edu. Res., 2026; 60(2):673-682.
https://www.ijper.org

Original Article

Conessine as A Novel Anti-Quorum Sensing Agent against *Streptococcus mutans*: An *in vitro* Analysis of Biofilm Inhibition

Khloud H Alsaadi*

Department of Biological Science, Science College, Jeddah University, Jeddah, SAUDI ARABIA.

ABSTRACT

Background: Dental caries concerns not solely the painful decay and eventual loss of the tooth but also significantly impacts an individual's physical, mental, and social health. The quest for potential Quorum Sensing (QS) inhibitors to hinder virulence, especially to mitigate the emergence of antibiotic resistance among caries pathogens, is increasing in this era of finding treatments from natural resources. **Objectives:** With the goal of finding a novel QS inhibitor, a plant alkaloid, conessine, has been evaluated for its inhibitory effect on biofilm formation, mature biofilm, and pathogen adherence against cariogenic *Streptococcus mutans*. **Materials and Methods:** The inhibitory effect of conessine on biofilm formation, as well as on developed biofilm was assessed using crystal violet assays. Colony-Forming Unit (CFU) counts on Mueller Hinton Agar were used to measure the inhibition of pathogen adhesion. Minimum Inhibitory Concentration (MIC) and Minimum Bactericidal Concentration (MBC) of conessine were determined using broth dilution assays. The live/dead cell analysis was performed using fluorescence microscopy, and quantitative Real-Time PCR (qRT-PCR) was employed to assess the expression of virulence genes StrepB and StrepgbpA. One-way ANOVA and Dunnett's test were used to analyze the statistical significance (p<0.001). **Results:** At the lower concentration (6.25±0.4 µg/mL) used in this study, conessine significantly inhibited biofilm formation and matured biofilm, with the inhibition rates of 23 and 29%, respectively. Adhesion was inhibited entirely at 100 µg/mL concentration of conessine. Conessine demonstrated the growth inhibition of *S. mutans*, with MIC_{50} at 31.811±2.01 µg/mL and MBC (IC_{90}) at 70.1252±3.56 µg/mL. Images from fluorescence microscopy confirmed *S. mutans* cell death at conessine MIC_{50}. Downregulation of StrepB and StrepgbpA genes, with the fold change 1.05 and 1.17, indicating the molecular mechanism behind reduced adherence and biofilm formation, respectively. **Conclusion:** This study is the first to demonstrate the potential anti-QS and anti-biofilm properties of conessine against *S. mutans in vitro*, suggesting it as a novel therapeutic agent for dental caries. Further investigations are needed to analyze the toxicity and optimize the anti-cariogenic properties at lower doses to assess clinical safety.

Keywords: Phytochemicals, Anti-Biofilm, Anti-caries, Virulence, Tooth Decay.

Correspondence:
Dr. Khloud H Alsaadi
Department of Biological Science, Science College, Jeddah University, Jeddah-23218, SAUDI ARABIA.
Email: khalsediy@uj.edu.sa

Received: 23-06-2025;
Revised: 18-08-2025;
Accepted: 08-11-2025.

INTRODUCTION

The WHO estimates that approximately 3.5 billion, or 50% of the global population, suffer from some form of oral health issues. According to the records in 2019, the prevalence of dental caries in permanent teeth is increasing in Saudi Arabia, with 86 and 65% cases reported in primary and permanent teeth, respectively.[1] In 1960, researchers identified *Streptococcus mutans* as the primary causative agent of dental disorders because it satisfied the criteria for infectivity as described in Koch's postulates.[2] Subsequently, studies revealed that Quorum Sensing (QS)/cell communication among *Streptococci, Veillonella* sp., and other initial colonizers raises an atmosphere favourable for secondary colonizers such as *Lactobacillus, Actinomyces*, and *Propionibacterium* species.[3] The deterioration of dental caries, due to the production of Extracellular Polymeric Substances (EPS) and acids from secondary pathogens, exacerbates oral health and leads to significant demineralization. Furthermore, the proliferation of late colonizers such as *Porphyromonas gingivalis* and *Candida albicans* facilitates matrix development and induces total degradation of dentin. Subsequent inflammation and deterioration of oral tissues lead to tooth loss.[3]

The goal of conventional treatment for dental caries is to protect tooth structure and avert further destruction. Though currently using non-invasive procedures efficiently delays or cures the risk factors of dental infection, side effects are still a major

DOI: 10.5530/ijper.20262947

concern. Recently, the search for plant-derived compounds or phytochemicals with therapeutic applications is growing with the aim of advancing sustainability. Organic chemists and industries welcome "Green Chemistry" concepts as an effort to reduce the use of harmful synthetic chemicals and chemical processes.[4] Phytochemicals, including alkaloids, terpenes, flavonoids, and others, contribute to the distinct properties of plants and exhibit a diverse array of therapeutic effects.[5] The remarkable contribution of phytochemicals from medicinal plants in the preparation of chemicals, cosmetics, and pharmaceutical drugs is widely recognized.[6] The availability of Conessine, a steroidal alkaloid, has been documented in various plant species, including *Holarrhena antidysenterica* Wall, *H. floribunda*, and *H. congolensis*.[7-10] In addition to its anaesthetic, insecticidal and antimalarial properties, conessine has demonstrated antibacterial efficacy against pathogenic *E. coli, Staphylococcus* sp., and *Bacillus* sp.[7,9,10-13] Conessine extracted from the plant species of Holarrhena has been reported to exhibit antibacterial efficacy against multidrug-resistant bacteria, including *Pseudomonas aeruginosa* and *Acinetobacter baumannii*, as evidenced by a few studies.[14] Conessine, derived from the Thai medicinal plant *Holarrhena antidysenterica*, enhanced the levofloxacin efficacy against multidrug-resistant *P. aeruginosa*.[8] The findings suggested that conessine may serve as an efflux pump inhibitor, reinstating antibiotic efficacy by impeding efflux pump mechanisms in *P. aeruginosa*.[15] The data suggested that conessine perhaps possess activity against other human pathogens. Hence, we aimed to investigate the anti-quorum sensing and antibiofilm efficacy of conessine against the cariogenic bacterium, *S. mutans. In vitro* studies were performed to investigate the anti-adherence, antibacterial, and anti-biofilm capabilities, as well as the influence of conessine on the expression profile of virulence genes was assessed by qRT-PCR analysis. This study presents the first report on the anti-quorum sensing/anti-biofilm efficacy of conessine on the cariogenic *S. mutans*.

MATERIALS AND METHODS

Preparation of test chemical and *S. mutans* culture for assays

S. mutans strain used in this study was acquired from King Fahad Hospital, Saudi Arabia and cultured to mid-log phase in Mueller Hinton Broth at 37°C with agitation (at 200 rpm) to prepare inoculum for *in vitro* assays. The growth of *S. mutans* in culture media was adjusted to a turbidity equivalent to 0.5% McFarland standard. Conessine compound was purchased from commercial supplier. Sterile deionized water was used to prepare varying concentrations of conessine for the assays.

Crystal violet assay

The inhibition of biofilm-forming *S. mutans* was evaluated by a modified method of crystal violet assay using a 96-well plate.[16] Each well received 200 µL of diluted inoculum, comprising 180 µL of sterile nutrient broth and 20 µL of standardized bacterial inoculum, and the plates were incubated at 37°C. After 72 hr, the wells were treated with different concentrations of conessine, viz 6.25, 12.5, 25, 50, and 100 µg/mL, and the control well was maintained without adding conessine. After incubation at 37°C for 24 hr, the wells were rinsed with sterile distilled water to remove planktonic bacterial cells and then air-dried at room temperature. Biofilm was stained with 200 µL of 1% (w/v) aqueous crystal violet solution for 20 M and the excess dye was removed by a distilled water rinse. The dried wells were added with 300 µL of DMSO to solubilize the adhered cells; further absorbance was read at 600 nm using a spectrophotometer.

Assay to investigate the inhibition of pre-formed biofilm

The inhibitory effect of conessine on the established or pre-formed *S. mutans* biofilm was investigated. Standardized *S. mutans* inoculum (20 µL) was added to the 96-well microtiter plate, which had already been filled with sterilized nutrient broth (100 µL).[17] The inoculated plate was incubated at 37°C for 72 hr to facilitate biofilm formation. 100 µL of fresh nutrient broth replaced the utilized broth, and conessine at varying concentrations (6.25, 12.5, 25, 50, and 100 µg/mL) was added to the test wells, and the control well was kept with inoculum (100 µL) and 5-10% DMSO. After incubation at 37°C for an additional 24 hr, the wells were rinsed thrice using sterile Phosphate-Buffered Saline (PBS, pH 7.4) to remove non-adherent cells. Biofilm in the dried plates (60°C for 30 m) was fixed by adding 100 µL of 95% ethanol (10 M), followed by staining with 5% (w/v) aqueous crystal violet solution. The Optical Density (OD) was measured using a microplate reader at 570 nm.

Analysis of the adherence inhibition efficacy

Adherence assay was performed to evaluate the inhibitory efficacy of conessine on the adhesion property of *S. mutans*.[18] Biofilm formation was facilitated in a 48-well plate as described earlier. The biofilm was treated with 25 and 100 µg/mL conessine, with the exception of the control, which was left untreated. After 24 hr of incubation, unadhered cells were removed by rinsing thrice with sterile distilled water, and the wells were air dried. Adhered cells were resuspended in 300 µL of sterile Phosphate-Buffered Saline (PBS), serially diluted up to 10^3, and kept at 37°C for 10 m to solubilize. The number of viable bacterial cells was quantified by the spread plate on Mueller Hinton Agar (MHA) and the Colony Forming Units (CFU) were expressed as CFU/mL.

Broth dilution assay to determine the Minimum Bactericidal Concentration (MIC)

MIC of conessine that displayed potent antimicrobial activity against *S. mutans* was evaluated by broth dilution assay.[19] 100 µL of two-fold diluted suspensions of *S. mutans* were added to wells of a microtiter plate, achieving a final volume of 200 µL per

well.[20] Varying concentrations (6.25, 12.5, 25, 50, and 100 µg/mL) of DMSO diluted conessine (1 mg/mL stock) was added to the wells, and the control was left untreated. MIC_{50} of conessine was obtained by measuring the absorbance (630 nm) using an ELISA Microplate Reader after 48 hr of incubation at 37°C. Growth inhibition in test wells was calculated using the following formula:

Percentage of inhibition = (OD of control - OD of test)/ (OD of control) × 100

Broth dilution assay to determine the Minimum Bactericidal Concentration (MBC)

MBC of conessine has been evaluated against *S. mutans* using a broth microdilution method followed by plating on MHA.[21] Two-fold dilutions of standardized stock inoculum, prepared as described above, were added to wells of a microtiter plate.[20] Conessine at increasing concentrations of 25, 50, and 100 µg/mL was introduced into the wells, except the control. After 24 hr of incubation at room temperature, 20 µL from each well was aseptically plated onto MHA, and the spread plates were incubated at 37°C for 48 hr. The MBC can be calculated by observing the lowest conessine concentration resulting in no growth or fewer than three colonies, corresponding to approximately 99-99.5% bacterial killing activity.

Fluorescence microscopy to evaluate live and dead cells of *S. mutans*

The staining solution for the live and dead assay was prepared by mixing equal volumes of SYTO 9 and propidium iodide in a microfuge tube.[22] SYTO 9 in the staining solution is absorbed by the live cells and appears in green fluorescence, and the dead cells stained with propidium iodide appear in red fluorescence. To experiment, pre-formed biofilms (as described earlier) in a 96-well microtiter plate were treated with 31.811 µg/mL (MIC_{50}) of conessine, whereas the control well was left untreated. After incubation at 37°C for 24 hr, each well was gently washed twice using sterile PBS to eliminate planktonic cells, then air-dried. Staining solution (3 µL) was added to all the wells and incubated at room temperature in a dark environment for 15 m. Excess stain was washed out with PBS, and the fluorescence was visualized using a fluorescence microscope (Olympus CKX41 equipped with an Optika Pro5 CCD camera).

Gene expression analysis by qRT-PCR

The expression of genes, StrepB and StrepgbpA, associated with virulence and biofilm formation in*S. mutans* was evaluated using quantitative Real-Time Polymerase Chain Reaction (qRT-PCR).[23] Biofilms, prepared as described in the above assays, were treated with the MIC_{50} of conessine, and the control well received no treatment. After 24 hr of incubation, total RNA was extracted from the biofilm formed in the conessine-treated *S. mutans* and control cultures, using the Total RNA Isolation Kit (Invitrogen, Cat# 10296010, USA) by following the manufacturer's instructions. The purity and concentration of RNA were quantified spectrophotometrically before complementary DNA (cDNA) synthesis, which was performed using iScript cDNA Synthesis Kit (Bio-Rad, Cat# 1708891). The reaction mixture was prepared using 1 µL of iScript Reverse Transcriptase, 0.5 µg of total RNA, 4 µL of 5× iScript reaction mix, and sterile distilled water to achieve the final volume of 20 µL. Thermal cycling conditions of priming at 25°C (5 M), cDNA synthesis at 46°C (20 M), and reverse transcriptase inactivation at 95°C (1 M) were set for one cycle in the Eppendorf Master Cycler.

qRT-PCR was performed to study the gene expression profile, using SYBR Green Master Mix (G Biosciences, Cat# 786-5062). Triplicates of reactions were performed in the LightCycler 96 system (Roche), and the data were analysed using the ΔΔCt method via LightCycler 96 SW 1.1 software. The primer sequences for StrepB and StrepgbpA genes used for amplification are given in Table 1. Reaction cycles, including initial activation at 95°C (2 M), 40 cycles of denaturation at 95°C (10 s), annealing at 58°C (1 M), and extension at 72°C (1 m/kb), and finally, a final hold at 4°C were set in the cycler. PCR products were analysed using 1.5% agarose gel electrophoresis, and the stained gel was visualized in the ChemiDoc Imaging System (Bio-Rad).

Statistical analysis

All assays were carried out in triplicate and the acquired data were expressed as mean values with the accompanying Standard Error (SE). SPSS software version 20.0 was used to perform the

Table 1: Forward and reverse primers used for qRT-PCR.

Genes	Primer sequences (5′ - 3′)		Annealing temperature
StrepB (StrepMgtfB)	F:	TACACTTTCGGGTGGCTTGG	67.0°C
	R:	AGAAGCTGTTTCCCCAACAGT	63.9°C
StrepgbpA (StrepMgbpA)	F:	TCATCAGGCACAGAACCACC	66.3°C
	R:	CAGTTGAGGCTCGTTTCCCT	65.5°C
16S	F:	CAGGCTTAGATACCCTGGTACTCC	64.4°C
	R:	CAGGATTAGATACCCTGGTACTCC	62.7°C

statistical analysis. One-way ANOVA followed by Dunnett's test was employed to validate significant inhibition (***p<0.001) relative to the control group across all tested concentrations.

RESULTS

Effect of conessine on the biofilm formation of *S. mutans* using the Crystal violet assay

The result of the Crystal violet assay demonstrated significant inhibition in the biofilm formation exhibited by *S. mutans* across all the tested doses of conessine in comparison to the untreated control (Figure 1). The lowest dose of 6.25 µg/mL of conessine used in this study exhibited a significant (***p<0.001) inhibition of the biofilm formation relative to the control. At the high doses of 50 and 100 µg/mL, an inhibition rate of 62 and 72% was observed, respectively.

Effect of conessine on the pre-formed biofilm of *S. mutans*

The disruptive effect of conessine on pre-formed biofilm of *S. mutans* was assessed, and the results are illustrated in Figure 2. A minimal dose of conessine at 6.25 µg/mL demonstrated 29% biofilm disruption with significant statistical difference (***p<0.001) compared to the control, indicating a strong biofilm disruptive effect exhibited even for the lowest dose of conessine used in this study. The highest biofilm disruption rate of 81% was observed when the conessine concentration was 100 µg/mL.

Effect of conessine on the adherence property of *S. mutans*

Conessine exhibited a dose-dependent inhibition of bacterial adhesion (Figure 3). The CFU estimated from the MHA plates indicated the quantity of viable adhered cells after conessine treatment. The control group (untreated) showed a viable bacterial count of 3.6×10^3 CFU/mL. Treatment using 25 µg/mL conessine against *S. mutans* significantly reduced the adhesion property, showing 0.4×10^3 CFU/mL of viable cells. At a high dose of 100 µg/mL, conessine completely inhibited the adhesion of *S. mutans*, resulting in no detectable colonies.

MIC of conessine against *S. mutans*

OD values at 630 nm revealed that Conessine demonstrated the growth inhibition of S. mutans in a dose-dependent manner, illustrated in Figure 4. The inhibition rates ranging from 27.15 to 75.16% were observed for the concentrations ranging from 6.25 to 100 µg/mL. Statistical analysis confirmed that low dose (6.25 µg/mL) of conessine exhibited significant inhibition (***p<0.001) of *S. mutans*, compared to the control group. The concentration of conessine required to inhibit 50% of bacterial growth (MIC_{50}) was determined using ED_{50} PLUS V1.0 software, and the value was 31.811 µg/mL.

MBC of conessine against *S. mutans*

The bacterial growth of 54.6×10^3 CFU/mL was observed from the control (untreated) MHA plates after incubation (Figure 5). Noticeable reduction in bacterial viability was observed at a lower concentration (25 µg/mL) of conessine, demonstrated 15×10^3

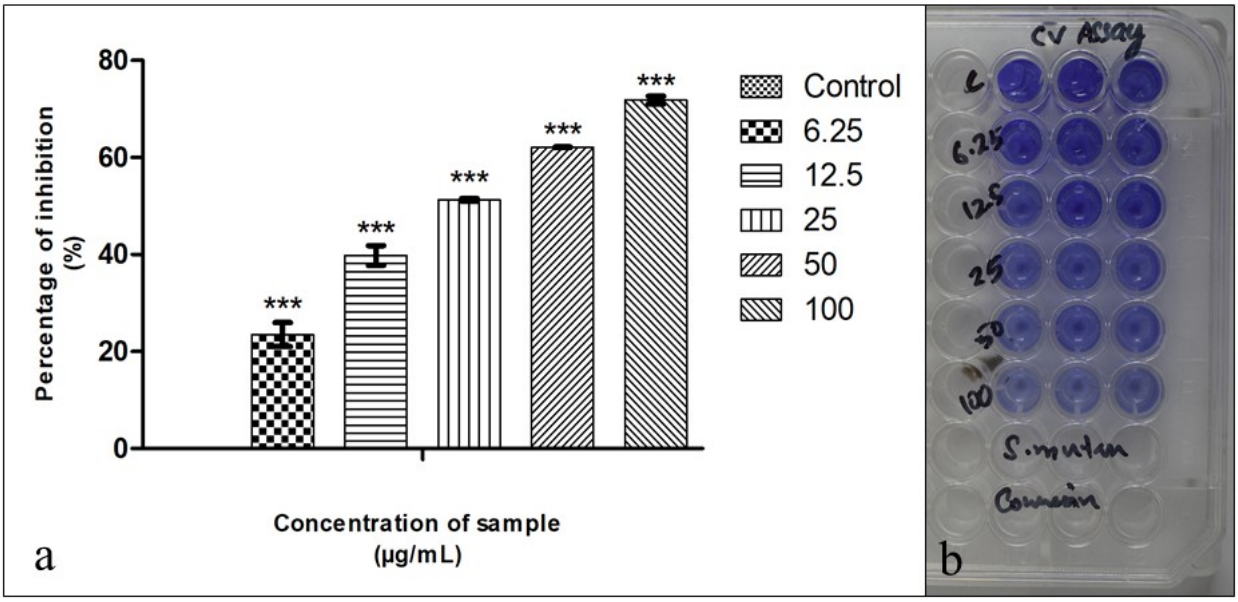

Figure 1: Result of Crystal violet assay demonstrates the antibiofilm effect of conessine against *S. mutans*. a - Bar diagram depicts the significant difference in the percentage of biofilm inhibition exhibited by control and varying test concentrations. Y axis - Percentage of inhibition; X axis - Varying concentration of conessine. b - Intensity of crystal violet stain in the wells shows the dose-dependent biofilm formation inhibition exhibited by conessine. All experiments were done in triplicates and results represented as Mean+/- SE. One-way ANOVA and Dunnett's test were performed to analyse data. ***p<0.001 compared to the control group.

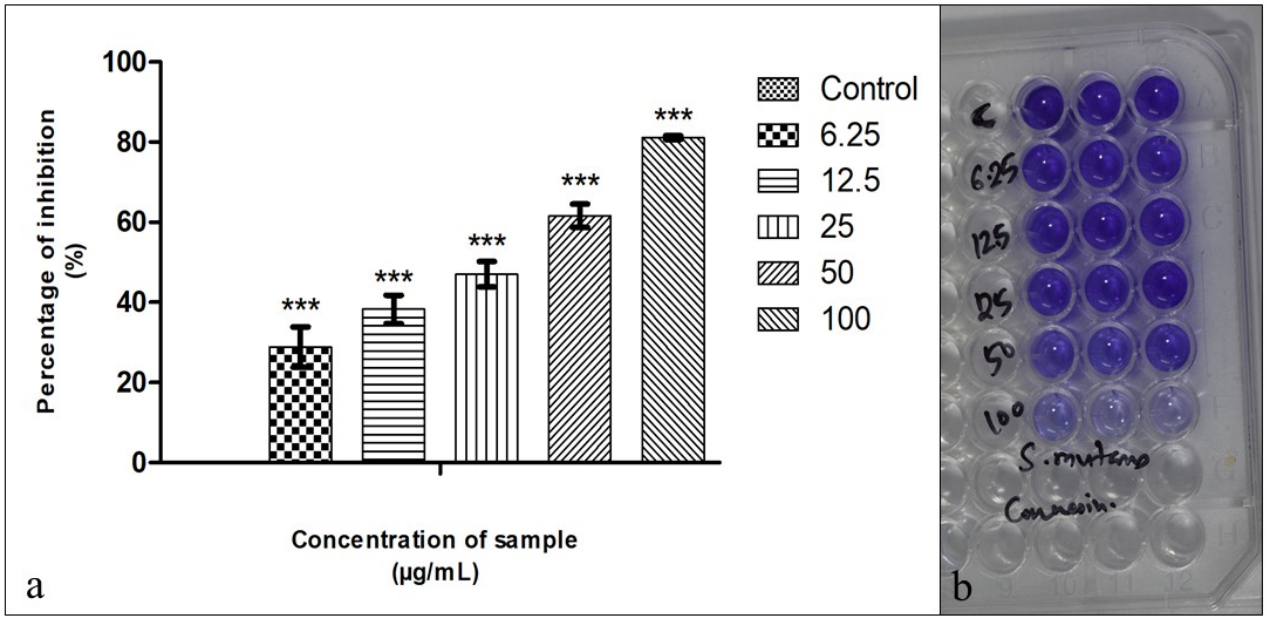

Figure 2: Result of biofilm inhibition assay shows the disruptive effect of conessine on the established biofilm of *S. mutans*. a - Bar diagram depicts significant difference between the tests and control. Y axis - Percentage of inhibition; X axis - Varying concentrations of conessine. b - Intensity of crystal violet stains shows the dose-dependent inhibitory effect of conessine. All experiments were done in triplicates and results represented as Mean+/- SE. One-way ANOVA and Dunnets test were performed to analyse data. ***p<0.001 compared to the control group.

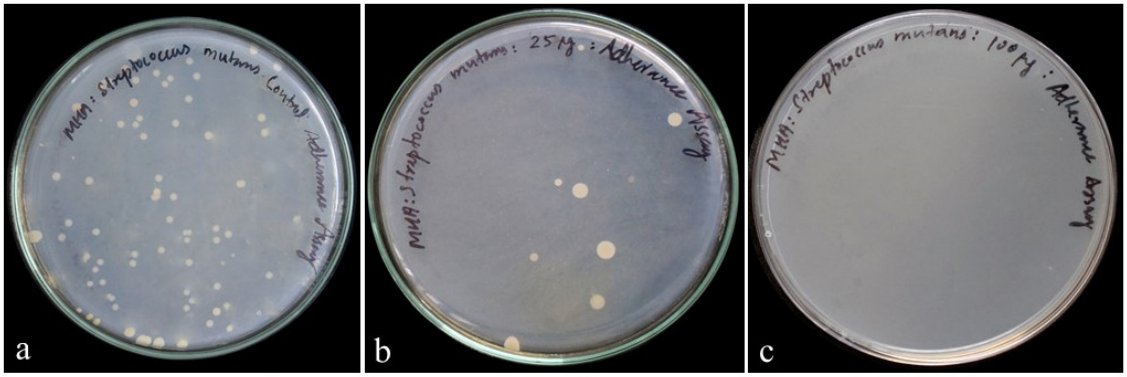

Treatment	Concentration (µg/ml)	No. of colonies	CFU/ml
Conessine	Control	72	$3.6*10^3$
	25	8	$0.4*10^3$
	100	0	-

Figure 3: Adherence inhibition efficacy exhibited by conessine against *S. mutans*. a, b, and c - Petri plates showing bacterial colony formation. a - control (without conessine treatment) showing dense growth of bacterium; b - Treated with conessine at 25 µg/mL concentration; c - Treated with conessine at 100 µg/mL concentration. The table shows number of colonies and CFU/mL obtained in this experiment.

CFU/mL viability, while 100 µg/mL concentration resulted in the bacterial viability of 0.45×10^3 CFU/mL. From this finding, complete nil growth or fewer than three colonies was not attained at the tested concentrations. However, the IC_{90} value, which denotes the dose of conessine required to inhibit 90% of *S. mutans* growth, was determined to be 70.1252 µg/mL, demonstrating a potential MBC value of conessine against *S. mutans*.

Effect of conessine to determine the live and dead cells after treatment

The fluorescence images demonstrated significant differences between treated and untreated samples (Figure 6). The control without conessine treatment showed a predominance of green fluorescence and less quantity of red, indicating a high proportion of live cells with intact membranes (Figures 6a and 6b). In contrast, the conessine-treated samples displayed a significant reduction in green fluorescence, but predominant

red fluorescence, suggesting a decrease in viable cells, indicative of compromised cell membranes (Figures 6c and 6d). These findings demonstrated that conessine at MIC_{50} effectively induces cell death in *S. mutans*.

Downregulation of virulence and biofilm associated gene expression in *S. mutans* by conessine treatment

qRT-PCR results revealed that conessine treatment significantly downregulated the expression of StrepB and StrepgbpA genes. The banding patterns observed in the gel image (Figure 7a) illustrate a suppression of both gene expressions compared to the control. In controls, the gene expression fold change was 1.0, considered as the baseline expression (Figures 7b and 7c), whereas conessine treatment significantly downregulated the expression of StrepB and StrepgbpA about 1.05 and 1.17-fold, respectively.

DISCUSSION

The growing threat of antimicrobial resistance and the adverse effects of conventional antibiotics cause significant challenges in drug discovery. Numerous natural compounds have been proven to possess anti-cariogenic properties until now. Beyond finding the anti-bacterial property, it is effective to find the natural QS inhibitors because they can block the QS-associated virulence pathways without exerting selective pressure on pathogens, thus mitigating the emergence of antibiotic resistance in pathogenic bacteria.[24] Despite various phytochemicals from plants have been documented for their anti-QS properties, the search for potential natural compounds continues as the prevalence of dental caries is increasing worldwide.[25,26] Hence, we have designed this novel study to investigate the anti-biofilm efficacy of plant alkaloid conessine against the initial colonizer of dental caries infection, *S. mutans*, via *in vitro* experiments.

The Crystal violet assay revealed that conessine significantly inhibits the biofilm formation of *S. mutans*, with inhibition rates ranging from 23 to 72% at the concentrations of 6.25 to 100 µg/mL. Similarly, in the biofilm inhibition assay, conessine significantly disrupted the pre-formed biofilms by the rate of 81% at 100 µg/mL concentration, highlighting its potential to target established biofilms, which are typically not affected by conventional treatments. According to reports, 500µM of curcumin exhibits approximately 75% biofilm inhibition against *S. mutans*.[27] Although the findings of our study indicate the dose-dependent effectiveness of conessine, it is mandatory to perform further research on the effectiveness of lower dosages.

Bacterial adhesion inhibition is a crucial step as it inhibits the initiation of biofilm formation, mediated by surface proteins and glucan production.[28] The adherence assay demonstrated complete inhibition at 100 µg/mL conessine concentration, which supports the anti-biofilm properties of conessine. Similar to the present study, dose-dependent adhesion inhibition was shown by curcumin against *S. mutans*.[29] Using 2X MIC (MIC: 15.62 µg/mL) of curcumin resulted in statistically decreased adherence of *S. mutans*. In our study, the MIC results showed that the IC_{50} of conessine against *S. mutans* was 31.811 µg/mL. In comparison to the MIC_{50} of natural plant-derived compounds such as quercetin and kaemferol against *S. mutans*, which were 16 and 8 mg/mL, respectively, our findings displayed improved inhibitory activity.[30] Antibacterial efficacy conessine containing *Holarrhena floribunda G. Don* was investigated against four species of

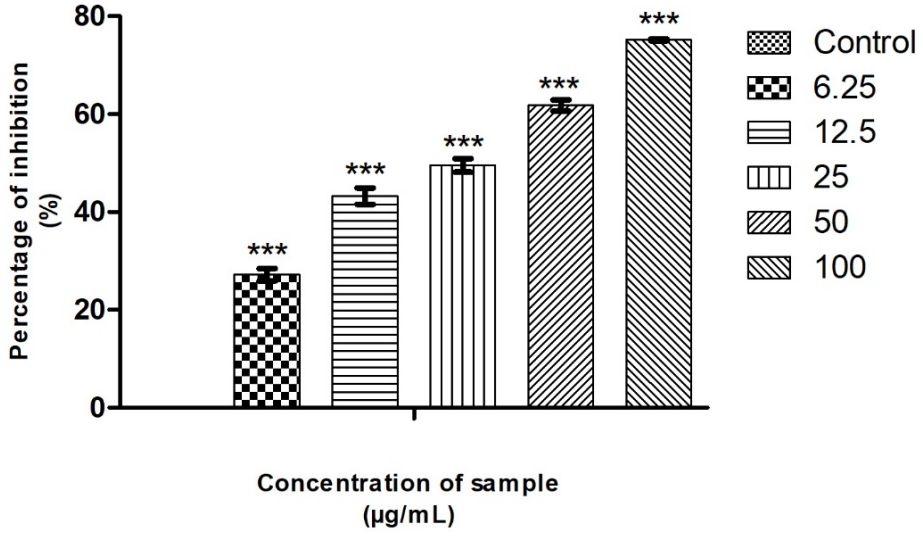

Figure 4: Graphical representation illustrating the Minimal Inhibitory Concentration (MIC) of conessine on *S. mutans*. Y axis - Percentage of inhibition; X axis - Varying concentration of conessine. All experiments were done in triplicates and results represented as Mean+/- SE. One-way ANOVA and Dunnets test were performed to analyse data. ***p<0.001 compared to control group. IC_{50} value of 31.811 µg/mL was recorded in this study.

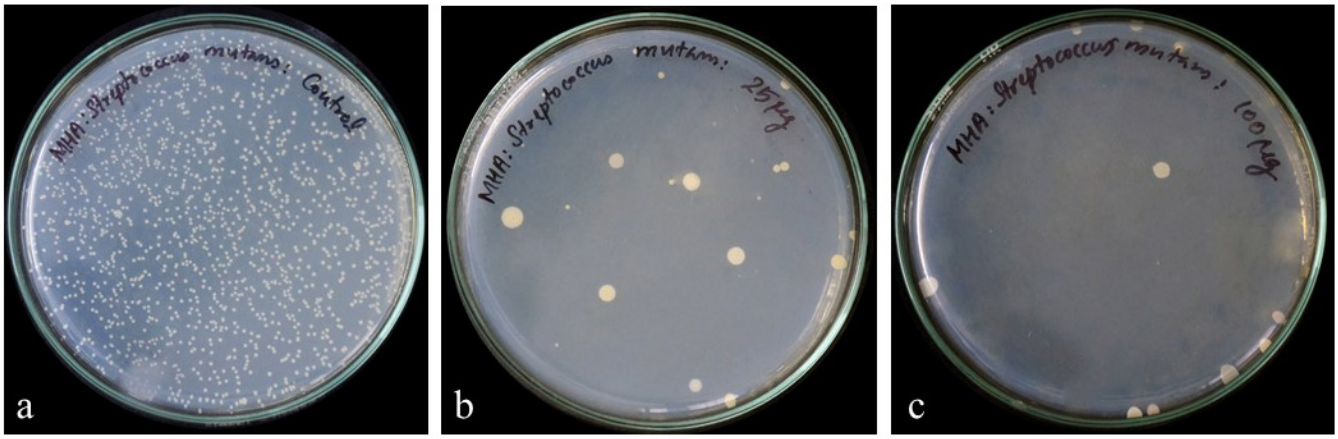

Figure 5: Petri plates showing the result of minimum bactericidal concentration of conessine against the biofilm forming *S. mutans*. a - Control (untreated) with 54.6*10^3 CFU/mL; b - Treated with conessine at 25 µg/mL concentration; c - Treated with conessine at 100 µg/mL concentration.

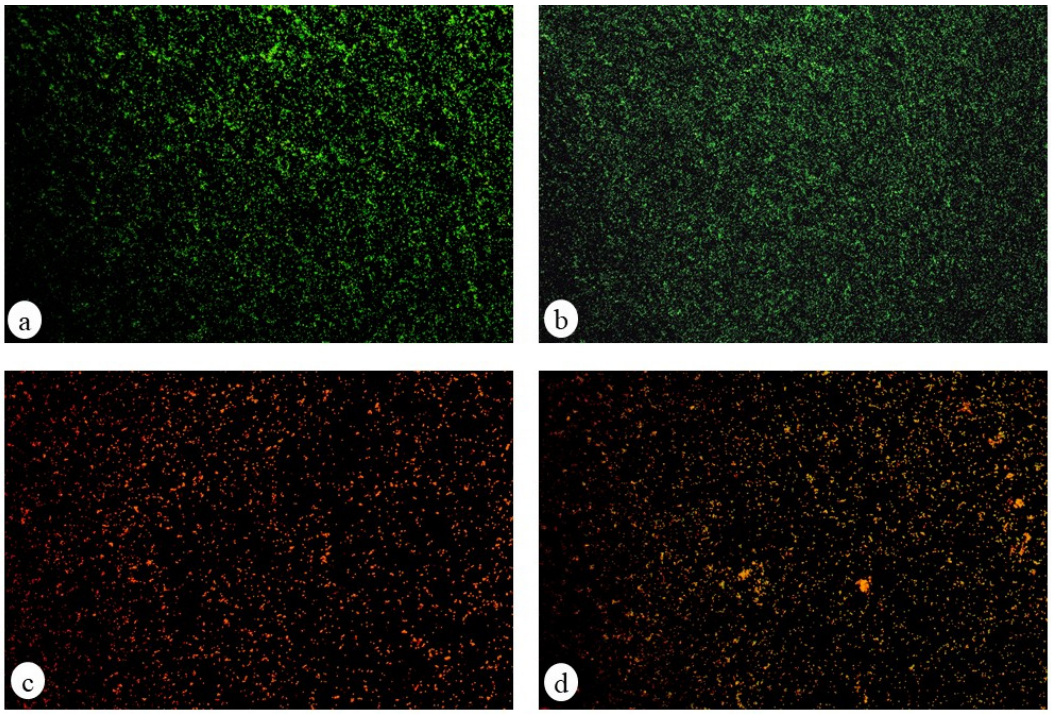

Figure 6: The fluorescence images demonstrate that conessine at MIC_{50} effectively induces cell death in *S. mutans*. a and b - The controls without conessine treatment show a predominance of green fluorescence and less quantity of red, indicating a high proportion of live cells with intact membranes. c and d - Conessine-treated samples display a significant reduction in green fluorescence, but predominant dead cells in red fluorescence.

Bacillus and observed that the MIC_{50} ranged from 50-150 µg/mL, whereas the MBC values were ranging from 105-280 µg/mL when the total alkaloid was used to test.[13] In Siriyong *et al*., study, conessine compound demonstrated the MIC value of 10 mg/L against *A. baumannii*.[14] In our study, the minimum concentration of conessine that is bactericidal (MBC) (IC_{90}) was 70.1252 µg/mL. Compared to the MBC values observed for curcumin against *S. mutans*, which was 62.5 µg/mL, the lower doses of conessine to kill 90% *S. mutans* are slightly higher, suggesting further investigation focussing of dosage and formulation are crucial for the safe and effective in inhibition of *S. mutans* colonization in the oral cavity.[29]

Live and dead assay results demonstrated the shift from live cells to dead cells following conessine treatment. Conessine treatment significantly reduced the biomass of live *S. mutans*. Moreover, the breakdown of cell membrane integrity revealed the interaction of conessine with lipid bilayers or membrane-bound proteins, which may collapse the cell membrane and result in the eradication of *S. mutans*.[31] Confocal Laser Scanning Microscopic (CLSM) images of curcumin-treated *S. mutans* biofilm showed a reduction in the live bacterial biomass and reduced biofilm thickness.[32] Reduction in the biofilm thickness leads to the deformation of the three-dimensional structure of biofilm, which may affect the cariogenic severity of *S. mutans*.[32]

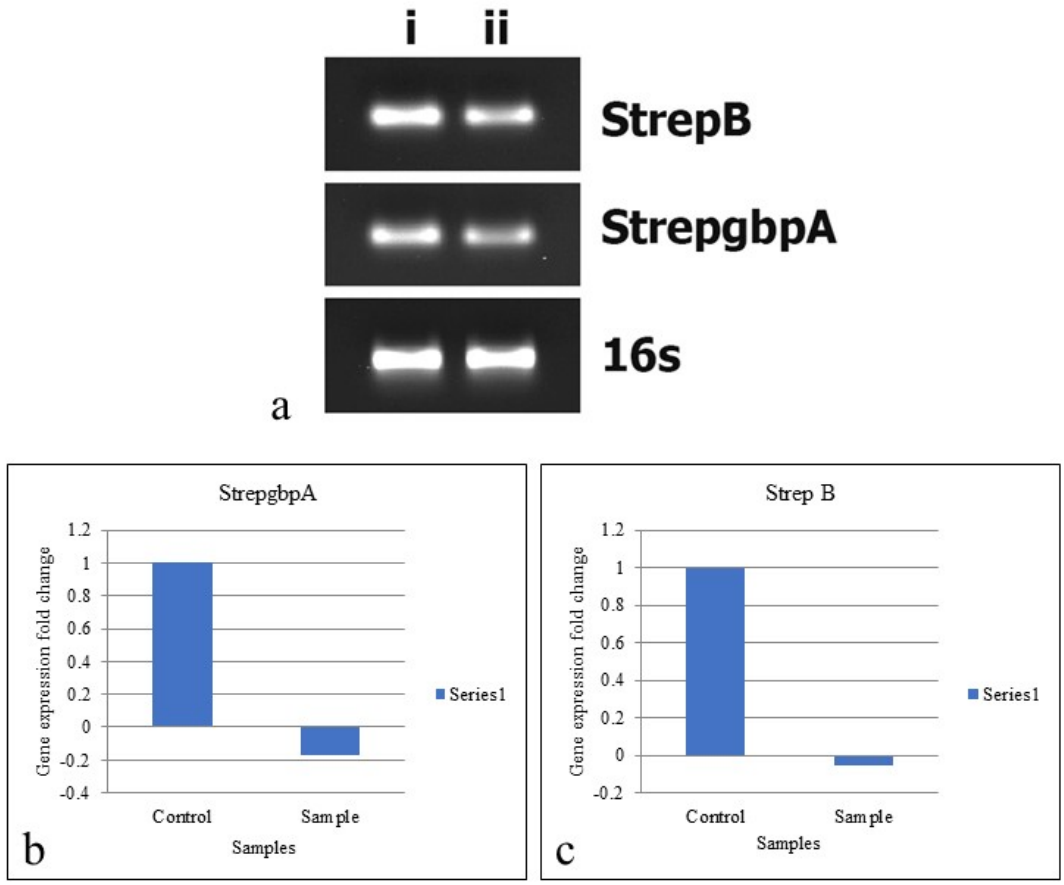

Figure 7: Gene expression analysis by qRT-PCR. a - Image of 1.5% agarose gel shows the expression profile of virulence genes in *S. mutans*, with 16S rRNA as reference gene. ai - Banding pattern demonstrates the expression of gene in control (untreated); aii - Banding patterns show the downregulated gene expression due to conessine (at MIC_{50}) treatment; b and c - Bar diagram demonstrate the fold change gene downregulation compared to control; b - Fold change in StrepgbpA expression; c - Fold change in StrepB expression.

A key finding of this study is the significant downregulation of virulence and biofilm-associated genes following conessine treatment at MIC_{50}. Considerable downregulation in the expression of StrepB and StrepgbpA genes impacts the molecular mechanisms supporting the pathogenicity of *S. mutans*, revealing a potential explanation for antibiofilm and anti-adhesion activity exhibited by conessine in the *in vitro* assays. StrepB (StrepMgtfB) gene is responsible for adhesion and accumulation of *S. mutans* on the tooth surface.[33] GtfB is one among the family of genes that code for glucosyltransferases (gtfs), which assist the sucrose-dependent adhesion in *S. mutans* on tooth surfaces. Gtfs breaks the sucrose into glucose and fructose, by forming the glycosidic linkage between the glucose moiety, a polymer of glucan termed as Extracellular Polysaccharides (EPSs) is developed. Gtfs can perform various catalytic functions and enhance the binding affinity to varying substrates due to signal peptides and variable domains in their structure. Hence, expression of gftB encourages bacterial adhesion and cell clustering, which results in the formation of plaque biofilms.[34] Downregulation of StrepB causes structural changes in the biofilm matrix and collapses bacterial resistance to host immune defence.[33] Significant downregulation of gtfB gene with 2.0 fold change was observed by the treatment of *Symplocarpus renifolius* extracts at 900 $\mu g \cdot mL^{-1}$ concentration.[35] In a study of Rudin *et al*., natural flavonoid, phloretin, was found to downregulate the expression of gtfB genes, which has been correlated with the reduced EPS content in *S. mutans*.[36]

Similar to gtfB, strepMgbpA (StrepgbpA) gene is known to facilitate cellular adhesion of *S. mutans* onto the tooth surface.[37] Gucan-binding proteins (gbp) gene is another family of genes with no known enzymatic activities like gtfs.[38] gbpA and gtfs shares some structural similarities as gbpA possesses domains for gtf enzymes, and additionally, it forms α-1,6 linkages for adhesion.[39] According to Banas *et al*., gbpA encourages the growth of taller microcolonies via α-1,6 linkages with glucan.[40] This was confirmed by the uniform layer of thin aggregated seen in the gbpA mutant of *S. mutans*, which demonstrating that the ratio of glucan and gbp is not sufficient for plaque development. Moreover, gbpA mutant *S. mutans* strains exhibited reduction of sucrose-dependant adhesion by 72-78%.[41] *S. mutans* possesses a variety of QS-associated virulence genes. In this study, the expression profile of virulence genes clearly demonstrated the downregulation of both StrepB and StrepgbpA, by showing 1.05 and 1.17 fold changes, respectively, indicating the potential

adhesion and biofilm disruption efficacy of conessine. The downregulation of these genes will affect the bacterial adhesion and subsequent biofilm formation onto the tooth surface. Moreover, the disruption of established biofilm affects the bacterial colonization, communication/QS, and virulence gene expression. Thus, conessine may act as a potential anti-QS compound that inhibits the biofilm formation of *S. mutans* in dental caries.

CONCLUSION

In conclusion, the results of the present study demonstrate the dose-dependent potential of anti-QS and anti-biofilm efficacy of conessine against *S. mutans in vitro*. These findings enhance the increasing interest in novel natural QSIs as alternatives to conventional antibiotics. Conessine can be developed as a new strategy to act against *Streptococcus mutans* which is a bacterium primarily responsible for dental caries. Additional research, particularly in *in vivo* models, is required to elucidate conessine's mechanisms of action against cariogenic bacteria, optimize its therapeutic potential at lower doses, and evaluate its safety for clinical applications in oral health.

ABBREVIATIONS

ANOVA: Analysis of Variance; **cDNA:** Complementary Deoxyribonucleic Acid; **CFU:** Colony-Forming Unit; **CLSM:** Confocal Laser Scanning Microscopy; **DMSO:** Dimethyl Sulfoxide; **EPS:** Extracellular Polymeric Substances; **MBC:** Minimum Bactericidal Concentration; **MHA:** Mueller Hinton Agar; **MIC:** Minimum Inhibitory Concentration; **OD:** Optical Density; **PBS:** Phosphate-Buffered Saline; **qRT-PCR:** Quantitative Real-Time Polymerase Chain Reaction; **QS:** Quorum Sensing; **RNA:** Ribonucleic Acid; **SE:** Standard Error; **StrepB (StrepMgtfB):** Glucosyltransferase B gene; **StrepgbpA (StrepMgbpA):** Glucan-Binding Protein A gene; **WHO:** World Health Organization.

CONFLICT OF INTEREST

The authors declare that there is no conflict of interest.

SUMMARY

Conessine, a steroidal alkaloid from plants like Holarrhena antidysenterica, was investigated for its anti-quorum sensing and anti-biofilm properties against Streptococcus mutans, a primary caries-causing bacterium. *In vitro* studies, including crystal violet assays, showed conessine significantly inhibited biofilm formation (23-72%) and disrupted mature biofilms (29-81%) at concentrations of 6.25-100 µg/mL. It completely blocked adhesion at 100 µg/mL and exhibited a MIC_{50} of 31.811 µg/mL and MBC (IC_{90}) of 70.1252 µg/mL. Fluorescence microscopy confirmed cell death, while qRT-PCR revealed downregulated StrepB and StrepgbpA genes, indicating reduced virulence. These findings suggest conessine's potential as a novel anti-caries therapeutic, warranting further clinical safety studies.

REFERENCES

1. Al-Rafee MA, AlShammery AR, Pani SC. A comparison of dental caries in urban and rural children of the Riyadh region of Saudi Arabia. Front Public Health. 2019; 7: 465826. doi: 10.3389/fpubh.2019.00195, PMID 31380359.
2. Gross EL, Leys EJ, Gasparovich SR, Firestone ND, Schwartzbaum JA, Janies DA, *et al.* Bacterial 16S sequence analysis of severe caries in young permanent teeth. J Clin Microbiol. 2010; 48(11): 4121-8. doi: 10.1128/JCM.01232-10, PMID 20826648.
3. Mysak J, Podzimek S, Sommerova P, Lyuya-Mi Y, Bartova J, Janatova T, et al. *Porphyromonas gingivalis*: major periodontopathic pathogen overview. J Immunol Res. 2014; 2014: 476068. doi: 10.1155/2014/476068, PMID 24741603.
4. Ramasubburayan R, Ramanathan G, Vijay SS, Angel SR, Ramya JR, Thirumurugan D, *et al.* Harnessing green nanoparticles: sustainable solutions for combating dental caries management. Mater Today Chem. 2025; 45: 102631. doi: 10.1016/j.mtchem.2025.102631.
5. Chaachouay N, Zidane L. Plant-derived natural products: A source for drug discovery and development. Drugs Drug Candidates. 2024; 3(1): 184-207. doi: 10.3390/ddc3010011.
6. Swami D, Anitha M, Rao MC, Sharangi A. Medicinal plants: perspectives and retrospectives. Med Plants. 2022: 1-28.
7. Thappa RK, Tikku K, Saxena BP, Vaid RM, Bhutani KK. Conessine as a larval growth inhibitor, sterilant, and antifeedant from *Holarrhena antidysenterica* Wall. Int J Trop Insect Sci. 1989; 10(2): 149-55. doi: 10.1017/S1742758400010304.
8. Siriyong T, Voravuthikunchai SP, Coote PJ. Steroidal alkaloids and conessine from the medicinal plant *Holarrhena antidysenterica* restore antibiotic efficacy in a *Galleria mellonella* model of multidrug-resistant *Pseudomonas aeruginosa* infection. BMC Complement Altern Med. 2018; 18: 285. doi: 10.1186/s12906-018-2350-8, PMID 30333003.
9. Dua VK, Verma G, Singh B, Rajan A, Bagai U, Agarwal DD, *et al.* Anti-malarial property of steroidal alkaloid conessine isolated from the bark of *Holarrhena antidysenterica*. Malar J. 2013; 12: 194. doi: 10.1186/1475-2875-12-194, PMID 23758861.
10. Burn JH. The action of conessine and holarrhenine the alkaloids of *Holarrhena congolensis*, and also of oxyconessine. J Pharmacol Exp Ther. 1915; 6(3): 305-21. doi: 10.1016/S0022-3565(25)08278-3.
11. Chakraborty A, Brantner AH. Antibacterial steroid alkaloids from the stem bark of *Holarrhena pubescens*. J Ethnopharmacol. 1999; 68(1-3): 339-44. doi: 10.1016/s0378-8741(99)00119-1, PMID 10624899.
12. Kavitha D, Shilpa P, Devaraj S. Antibacterial effect of conessine, an alkaloid from *Holarrhena antidysenterica*, against enteropathogenic Escherichia coli. Indian J Pharm Educ Res. 2003; 37(2): 85-9.
13. Patrice K, Véronique PB, David L, François-Xavier E. Antibacterial activities of the extracts and conessine from *Holarrhena floribunda* G. Don. (Apocynaceae). Afr J Tradit Complement Altern Med. 2007; 4(3): 352-6. doi: 10.4314/ajtcam.v4i3.31233, PMID 20161901.
14. Siriyong T, Chusri S, Srimanote P, Tipmanee V, Voravuthikunchai SP. *Holarrhena antidysenterica* extract and its steroidal alkaloid, conessine, as resistance-modifying agents against extensively drug-resistant *Acinetobacter baumannii*. Microb Drug Resist. 2016; 22(4): 273-82. doi: 10.1089/mdr.2015.0194, PMID 26745443.
15. Siriyong T, Srimanote P, Chusri S, Yingyongnarongkul BE, Suaisom C, Tipmanee V, *et al.* Conessine as a novel inhibitor of multidrug efflux pump systems in *Pseudomonas aeruginosa*. BMC Complement Altern Med. 2017; 17(1): 405. doi: 10.1186/s12906-017-1913-y, PMID 28806947.
16. Kugaji MS, Kumbar VM, Peram MR, Patil S, Bhat KG, Diwan PV. Effect of resveratrol on biofilm formation and virulence factor gene expression of *Porphyromonas gingivalis* in periodontal disease. APMIS. 2019; 127(4): 187-95. doi: 10.1111/apm.12915, PMID 30737899.
17. Migliaccio A, Stabile M, Triassi M, Dé E, De Gregorio E, Zarrilli R. Inhibition of biofilm formation and preformed biofilm in *Acinetobacter baumannii* by resveratrol, chlorhexidine and benzalkonium: modulation of efflux pump activity. Front Microbiol. 2024; 15: 1494772. doi: 10.3389/fmicb.2024.1494772, PMID 39736993.
18. Xiong K, Chen X, Hu H, Hou H, Gao P, Zou L. Antimicrobial effect of a peptide containing novel oral spray on *Streptococcus mutans*. BioMed Res Int. 2020; 2020: 6853652. doi: 10.1155/2020/6853652, PMID 32258136.
19. Cho E, Hwang JY, Park JS, Oh D, Oh DC, Park HG, *et al.* Inhibition of *Streptococcus mutans* adhesion and biofilm formation with small-molecule inhibitors of sortase A from Juniperus chinensis. J Oral Microbiol. 2022; 14(1): 2088937. doi: 10.1080/20002297.2022.2088937, PMID 35756538.
20. Buwa LV, van Staden J. Antibacterial and antifungal activity of traditional medicinal plants used against venereal diseases in South Africa. J Ethnopharmacol. 2006; 103(1): 139-42. doi: 10.1016/j.jep.2005.09.020, PMID 16271287.
21. Swebocki T, Barras A. Kocot AM. Minimum Inhibitory Concentration (MIC) and Minimum Bactericidal Concentration (MBC) assays using broth microdilution method. Methods Mol Biol. 2023; 2620: 183-90. doi: 10.1007/978-1-0716-2942-0_18, PMID 37081158.

22. Cai Y, Strømme M, Welch K. Bacteria viability assessment after photocatalytic treatment. 3 Biotech. 2014; 4(2): 149-57. doi: 10.1007/s13205-013-0137-1, PMID 28324445.
23. Argimón S, Caufield PW. Distribution of putative virulence genes in *Streptococcus mutans* strains does not correlate with caries experience. J Clin Microbiol. 2011; 49(3): 984-92. doi: 10.1128/JCM.00829-10, PMID 21214109.
24. Zhou L, Zhang Y, Ge Y, Zhu X, Pan J. Regulatory mechanisms and promising applications of quorum sensing-inhibiting agents in control of bacterial biofilm formation. Front Microbiol. 2020; 11: 589640. doi: 10.3389/fmicb.2020.589640, PMID 33178172.
25. Moktan N, Gajbhiye RL, Sahithi TV, Roy DN, Kundu R, Banerjee A. Antibacterial and antibiofilm activities of extract and bioactive compounds from *Bergenia ciliata* (Haw.) Sternb. flowers against *Streptococcus mutans* through cell membrane damage. J Ethnopharmacol. 2025; 339: 119144. doi: 10.1016/j.jep.2024.119144, PMID 39577678.
26. Pallavi P, Sahoo PP, Sen SK, Raut S. Comparative evaluation of anti-biofilm and anti-adherence potential of plant extracts against *Streptococcus mutans*: A therapeutic approach for oral health. Microb Pathog. 2024; 188: 106514. doi: 10.1016/j.micpath.2023.106514, PMID 38296118.
27. Li B, Li X, Lin H, Zhou Y. Curcumin as a promising antibacterial agent: effects on metabolism and biofilm formation in S. mutans. BioMed Res Int. 2018; 2018: 4508709. doi: 10.1155/2018/4508709, PMID 29682545.
28. Sharma S, Mohler J, Mahajan SD, Schwartz SA, Bruggemann L, Aalinkeel R. Microbial biofilm: a review on formation, infection, antibiotic resistance, control measures, and innovative treatment. Microorganisms. 2023; 11(6): 1614. doi: 10.3390/microorganisms11061614, PMID 37375116.
29. Kumbar VM, Peram MR, Kugaji MS, Patil S, Kambimath M, Magennavar S, *et al.* Antimicrobial and antibiofilm activity of curcumin against oral pathogens: potential for periodontal treatment. Microbe. 2025; 7: 100355. doi: 10.1016/j.microb.2025.100355.
30. Zeng Y, Nikitkova A, Abdelsalam H, Li J, Xiao J. Activity of quercetin and kaemferol against *Streptococcus mutans* biofilm. Arch Oral Biol. 2019; 98: 9-16. doi: 10.1016/j.archoralbio.2018.11.005, PMID 30419487.
31. Bottner A, He RY, Sarbu A, Nainar SM, Dufour D, Gong SG, et al. *Streptococcus mutans* isolated from children with severe-early childhood caries form higher levels of persisters. Arch Oral Biol. 2020; 110: 104601. doi: 10.1016/j.archoralbio.2019.104601, PMID 31734540.
32. Li B, Pan T, Lin H, Zhou Y. The enhancing antibiofilm activity of curcumin on *Streptococcus mutans* strains from severe early childhood caries. BMC Microbiol. 2020; 20: 286. doi: 10.1186/s12866-020-01967-2, PMID 32957947.
33. Zhang Q, Ma Q, Wang Y, Wu H, Zou J. Molecular mechanisms of inhibiting glucosyltransferases for biofilm formation in *Streptococcus mutans*. Int J Oral Sci. 2021; 13: 30. doi: 10.1038/s41368-021-00132-x, PMID 34465766.
34. Simón-Soro A, Mira A. Solving the etiology of dental caries. Trends Microbiol. 2015; 23(2): 76-82. doi: 10.1016/j.tim.2014.10.010, PMID 25435135.
35. Lee YC, Cho SG, Kim SW, Kim JN. Anticariogenic potential of Korean native plant extracts *against Streptococcus mutans*. Planta Med. 2019; 85(16): 1242-52. doi: 10.1055/a-1013-2154, PMID 31689774.
36. Rudin L, Bornstein MM, Shyp V. Inhibition of biofilm formation and virulence factors of cariogenic oral pathogen *Streptococcus mutans* by natural flavonoid phloretin. J Oral Microbiol. 2023; 15(1): 2230711. doi: 10.1080/20002297.2023.2230711, PMID 37416858.
37. Tamanna IS, Smiline Girija A, Priyadharshini JV. Detection of gbpA and gbpB in *Streptococcus mutans* isolated from patients with oral potentially malignant disorders: A pilot study. J Clin Diagn Res. 2024; 18(7): DC06-10. doi: 10.7860/JCDR/2024/69823.19647.
38. Sato Y, Yamamoto Y, Kizaki H. Cloning and sequence analysis of the gbpC gene encoding a novel glucan-binding protein of *Streptococcus mutans*. Infect Immun. 1997; 65(2): 668-75. doi: 10.1128/iai.65.2.668-675.1997, PMID 9009329.
39. Bowen WH, Koo H. Biology of *Streptococcus mutans*-derived glucosyltransferases: role in extracellular matrix formation of cariogenic biofilms. Caries Res. 2011; 45(1): 69-86. doi: 10.1159/000324598, PMID 21346355.
40. Banas JA, Fountain TL, Mazurkiewicz JE, Sun K, Vickerman MM. *Streptococcus mutans* glucan-binding protein-A affects *Streptococcus gordonii* biofilm architecture. FEMS Microbiol Lett. 2007; 267(1): 80-8. doi: 10.1111/j.1574-6968.2006.00557.x, PMID 17166223.
41. Hazlett KR, Michalek SM, Banas JA. Inactivation of the gbpA gene of *Streptococcus mutans* increases virulence and promotes *in vivo* accumulation of recombinations between the glucosyltransferase B and C genes. Infect Immun. 1998; 66(5): 2180-5. doi: 10.1128/IAI.66.5.2180-2185.1998, PMID 9573105.

Cite this article: Alsaadi KH. Conessine as A Novel Anti-Quorum Sensing Agent against *Streptococcus mutans*: An *in vitro* Analysis of Biofilm Inhibition. Indian J of Pharmaceutical Education and Research. 2026;60(2):673-82.